JOURNAL OF MATERIALS SCIENCE 23 (1988) 3678–3682

TEM study of the disorder–order perovskite, $Pb(In_{1/2}Nb_{1/2})O_3$

C. A. RANDALL*, D. J. BARBER
Department of Physics, University of Essex, Wivenhoe Park, Colchester, UK

P. GROVES
Clarendon Laboratory, Parks Road, Oxford, UK

R. W. WHATMORE
Allen Clark Research Centre, Towcester, UK

A transmission electron microscopy study of the order–disorder perovskite $Pb(In_{1/2}Nb_{1/2})O_3$ (PIN) has shown that its microstructures are dependent on the In : Nb B-site cation distribution. In disordered PIN the dielectric properties are those of a relaxor ferroelectric. Lowering the temperature of disordered PIN by means of a liquid nitrogen-cooled stage has been found to stabilize polar ferroelectric micro-domains, ~20 to 30 nm in size. On increasing the long-range order of the B-site cations to give ordered domains > 80 nm in size, an antiferroelectric phase is shown to develop that is isostructural with the antiferroelectric perovskite, $PbZrO_3$. Coexisting antiferroelectric and non-antiferroelectric regions have been observed in partially ordered PIN.

1. Introduction

Many complex perovskite compounds corresponding to the general formula, $A(B'B'')O_3$, have a diffuse phase transition which is frequency dependent in the ratio-frequency range. These materials form a subgroup of the ferroelectrics and are known as relaxor ferroelectrics. Smolenskii and co-workers [1–3] pointed out that this relaxor behaviour was a direct consequence of nanoscale compositional fluctuations. Two independent studies by Setter and Cross [4, 5] and Stenger and Burggraaf [6, 7] showed the importance of local chemical fluctuations by means of disorder–order experiments on the perovskites $Pb(Sc_{1/2}Ta_{1/2})O_3$ (PST) and $Pb(Sc_{1/2}Nb_{1/2})O_3$ (PSN). From these studies the key-role of the distribution of the B-site cations in determining the observed dielectric and optical behaviour was established. In disordered PST a broad phase transition is observed with a frequency dependent (relaxor-type) relationship between permittivity and temperature. However, in highly ordered PST a sharp transition with little frequency dependence is obtained, indicative of a more "normal" ferroelectric transition.

As the temperature of a relaxor crystal is lowered, individual microregions undergo the paraelectric–ferroelectric transition and the crystal develops a spontaneous polarization in which localized dipole alignments lead to polar microdomains. The behaviour of the spontaneous dipole polarization can be qualitatively understood by analogy with the behaviour of a superparamagnet as suggested by Cross [8] and Cross *et al.* [9]. The height of the energy barrier, ϕ, between degenerate dipole states is proportional to the volume of the polar microdomains. When the thermal energy, $k_B T$ exceeds or is of the order of ϕ, the dipoles are subject to thermal agitation so that their orientations will flip between degenerate directions. Reducing the thermal energy so that $k_B T$ is less than ϕ causes the dipoles to be "frozen" into one of the possible polar directions. Recently, Yokosuka and Marutake [10] have developed a semi-quantitative model for relaxor ferroelectrics with rotatable dipoles in ferroelectric polar microdomains. The predictions of this model show good correlation with experimental dielectric results.

A number of studies have been performed on the complex disorder–order perovskite $Pb(In_{1/2}Nb_{1/2})O_3$. When PIN is disordered, broad relaxor ferroelectric characteristics are observed [11–13]. Annealing at ~700° C for several hours causes the In : Nb cations to order sufficiently on the B-sites to produce a normal antiferroelectric perovskite-structured PIN, observed by Groves [13] and Turik *et al.* [15]. The antiparallel dipole ordering of this antiferroelectric PIN phase is isostructurally related to the antiferroelectric superstructure of $PbZrO_3$ [13].

2. Experimental details

2.1. Preparation of materials

2.1.1. Single crystals

Single crystals of PIN were grown in a PbO-flux [13]. The single crystals were green in colour, with a cuboid shape, and their sides measured as ~0.5 to 1.0 mm. Because the crystals were very small they were only used for experiments designed to confirm results obtained from polycrystalline materials.

* *Present address*: Materials Research Laboratory, The Pennsylvania State University, University Park, Pennsylvania 16802, USA.

0022–2461/88 $03.00 + .12

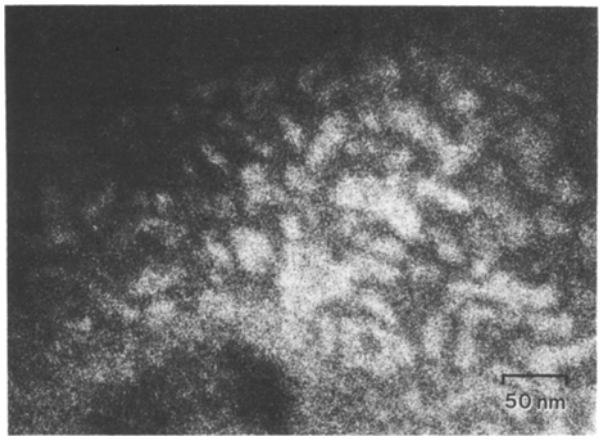

Figure 1 Dark-field image formed using an F-type (order) reflection revealing the ordered domains in unannealed relaxor ferroelectric PIN ceramic (recorded on X-ray film).

2.1.2. Hot-pressed ceramics

A common problem in the synthesis of complex lead-based perovskites is the production of an unwanted pyrochlore phase. The presence of pyrochlore is undesirable because it impairs the dielectric properties of the perovskite ceramics. The best known method of inhibiting pyrochlore formation was suggested by Swartz and Shrout [16]. In this process a separate B-site precursor reaction takes place, e.g.

$$In_2O_3 + Nb_2O_5 \rightarrow 2(InNb)O_4$$

In the case of PIN, a Wolframite-structured B-site precursor is produced and this is subsequently reacted with lead oxide to form the required perovskite phase, after Groves [16]

$$2PbO + InNbO_4 \rightarrow Pb_2(InNb)O_6$$

The success of the Swartz–Shrout method depends on both intrinsic material properties and processing parameters, which include the reactivity of In_2O_3, the achievement of homogeneous mixing and adequate control over volatilization of PbO from the reactants.

2.2. Preparation for TEM

Thin slices of both unannealed and annealed ceramics and single crystals were polished to a thickness $\sim 30\,\mu m$ and then mounted on copper grids with epoxy resin. These specimens were then ion-beam thinned, using beams of 5 keV argon atoms incident at angles of 18 to 20°. Low beam intensities were employed to minimize heating and thus reduce the possibility of loss of volatiles (chiefly lead oxide).

2.3. TEM techniques

Transmission electron microscopy (TEM) was carried out on a Jeol-200CX microscope fitted with a Hexland liquid nitrogen cooled-stage. The temperature, T^*, indicated by the thermocouple meter supplied with the stage, is always likely to differ from the temperature of an area undergoing analysis because of competition between electron-beam heating effects and the thermal conduction through the specimen.

When low-temperature phase transitions give rise to weak superstructure reflections, it is difficult to record dark-field (DF) images using these reflections because of specimen drift during the long times that are needed to record images on film. Increasing the intensity of the incident electron beam causes the local specimen temperature to rise and this reduces the intensities of the superstructure diffraction spots. It was therefore found to be advantageous to use fast, high-contrast, X-ray film to record DF images formed in this way. Despite the lower resolution of the X-ray emulsion this procedure was beneficial for most purposes.

3. Results

3.1. Ferroelectric relaxor disordered $Pb(In_{1/2}Nb_{1/2})O_3$

In disordered PIN (both ceramics and single crystals) the In : Nb distribution gives rise to small ordered regions, ~ 30 nm in size, and the dielectric behaviour shows a diffuse phase transition. The 30 nm ordered

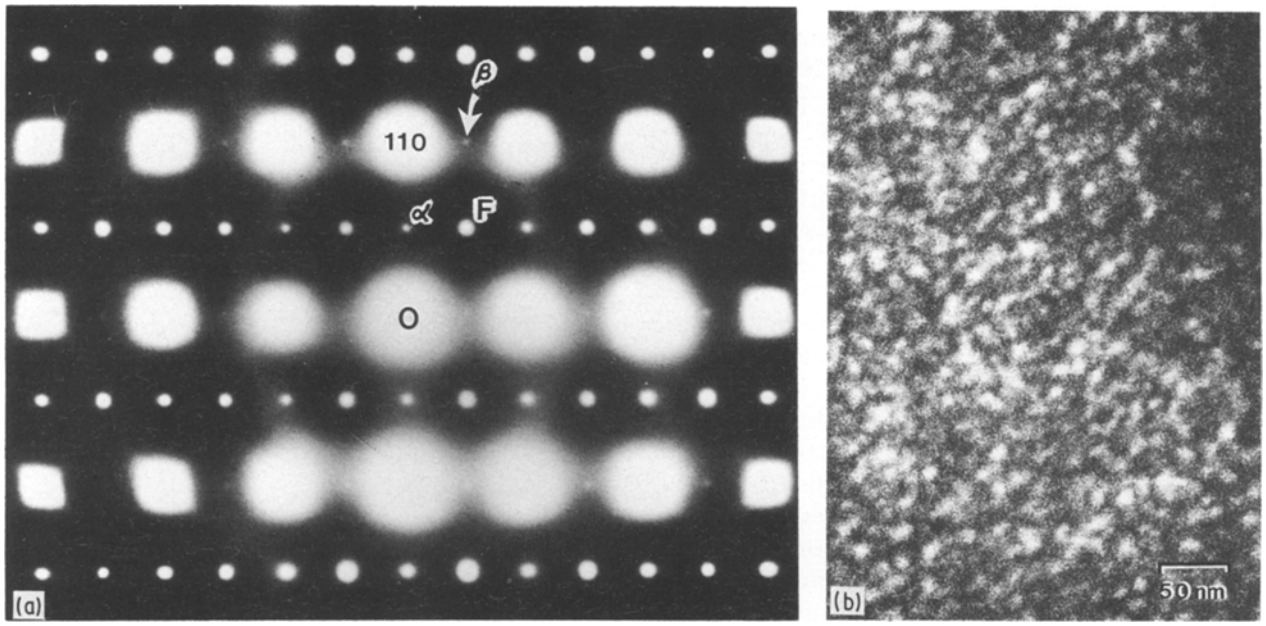

Figure 2 (a) ⟨1 1 0⟩ zone axis diffraction pattern from disordered PIN, recorded at liquid nitrogen temperatures. Weak α-, β- and F-type reflections are indicated. (b) Dark-field image of disordered PIN, recorded using a weak superstructure spot of type 3/2, 1/2, 0 at liquid nitrogen temperatures.

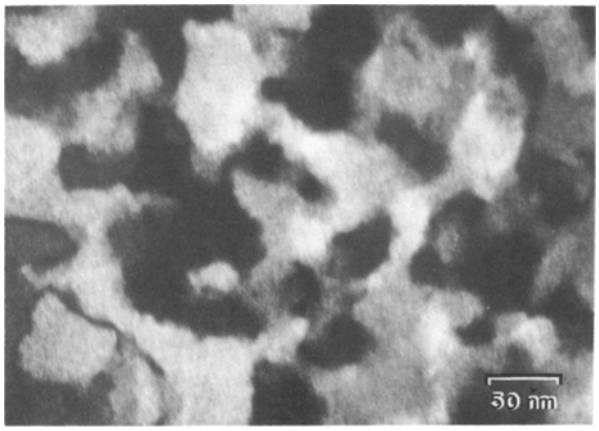

Figure 3 Dark-field image recorded using an F-type spot revealing large ordered domains in annealed-PIN ceramic.

domains can be directly revealed by DF imaging using one of the superstructure diffraction spots (so-called F-type spots) arising from the ordered structure. Fig. 1 shows the contrast of the ordered domains in disordered PIN; the dark and light regions are of weaker contrast than those observed in $Pb(Sc_{1/2}Ta_{1/2})O_3$ but are qualitatively similar [18].

Reducing the temperature by some 170 K by means of the liquid nitrogen-cooled specimen stage induces additional diffraction spots of type $\{h + 1/2, k + 1/2, 0\}$ and $\{h + 1/2, 0, 0\}$ (otherwise known as α and β spots), similar to those found in the ferroelectric state of PST [18]. In the case of PIN, the β-type superstructure spots in the $\langle 1\,1\,0\rangle$ zone axis diffraction pattern are very much weaker relative to the α-type superlattice spots than for PST. Both types of spot are visible in Fig. 2a. These superlattice reflections have been attributed to the ordered-B-site sublattice modulating dipole displacements of the ions on the A-site sublattice to produce inequivalent displacements on adjacent lead sites [18, 19]. DF imaging using a $\boldsymbol{g} = 3/2, 1/2, 0$ reciprocal lattice vector at these low temperatures reveals a weak domain contrast associated with stable polar microdomains [19]. Fig. 2b shows a DF image of low contrast, mottled domain configurations, the domains being ~ 30 nm diameter. However, these stabilized polar microdomains could not be switched *in situ* to a macrodomain state, as is found to be possible in PLZT [20].

3.2. Antiferroelectric $Pb(In_{1/2}Nb_{1/2})O_3$

Annealing PIN for over 20 h at 700° C induces long-range order of the indium and niobium ions to an extent such that the compositional fluctuations are very much reduced and a sharper phase transition occurs. However, unlike the case of ordered PST, where the low temperature phase is ferroelectric, in ordered PIN it shows an antiferroelectric behaviour [13–15]. The antiferroelectric structure begins to appear once the ordered domains reach a size > 80 nm. Fig. 3 shows a DF image formed using an F-type (order) superstructure spot to reveal the ordered domains > 100 nm in size in antiferroelectric PIN ceramic. The electron diffraction patterns from antiferroelectric PIN shows superstructure spots of type $\{h/4, k/4, 0\}$ associated with antiparallel dipole

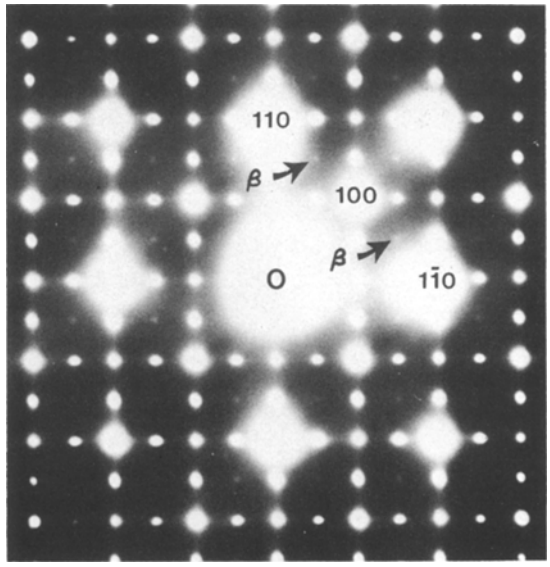

Figure 4 A selected-area $\langle 1\,0\,0\rangle$ zone axis electron diffraction from a region containing a 90° domain boundary in antiferroelectric PIN. Note also the presence of weak β-type superstructure spots which are not associated with the antiferroelectric PIN.

ordering. Fig. 4 shows a selected-area $\langle 1\,0\,0\rangle$ zone axis diffraction pattern recorded with the field aperture across a 90° domain boundary, the results being very similar in appearance to the observations made on the antiferroelectric perovskite $PbZrO_3$ by Tanaka *et al.* [21], but with additional β-type superstructure spots. The antiferroelectric dipole ordering is schematically represented in Fig. 5. The macro-twin-like domains are shown in Fig. 6a; within each domain is a fine scale contrast. By DF imaging using an antiferroelectric superstructure spot $\{h/4, k/4, 0\}$ this contrast is revealed to be caused by microdomains, as demonstrated in Fig. 6b. In a DF image formed using an antiferroelectric diffraction spot the light regions

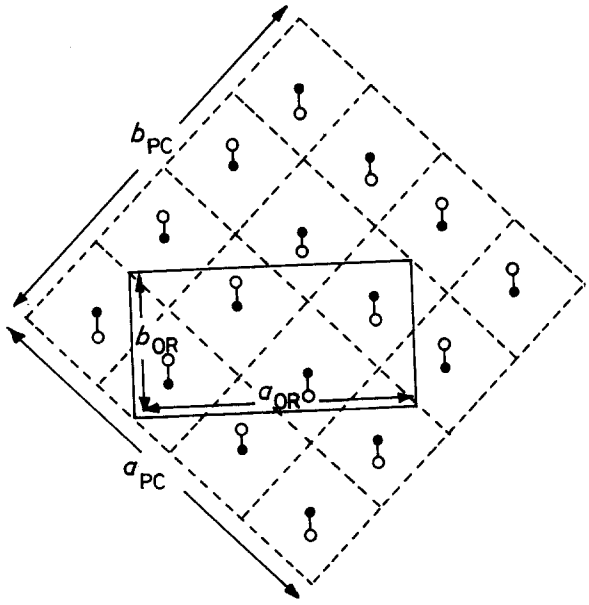

Figure 5 Schematic representation of the cation displacements in antiferroelectric PIN, after Groves [13, 14]. The subscript PC refers to the pseudo-cubic cell, and the subscript OR refers to the simplest orthorhombic cell, outlined in the projection.

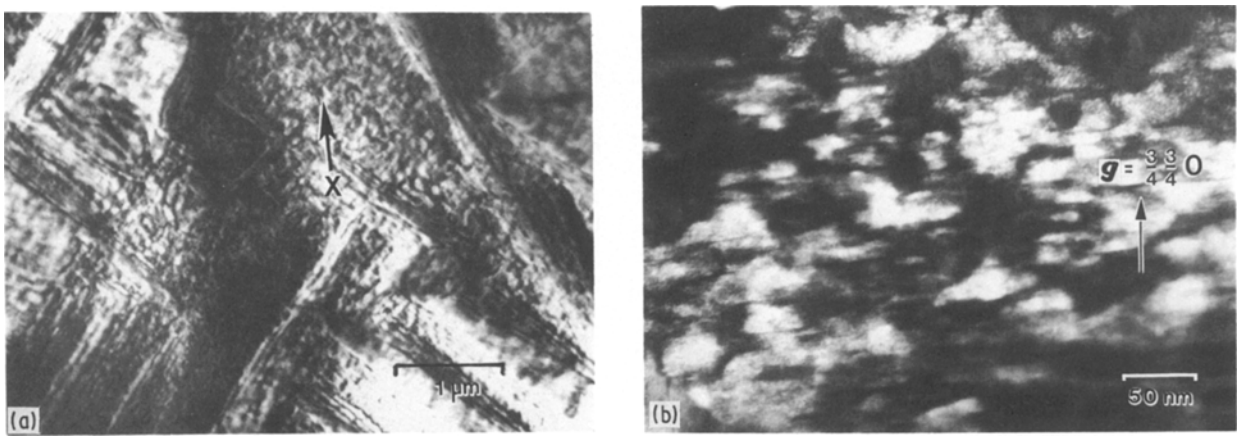

Figure 6 (a) Bright-field micrograph showing typical antiferroelectric macrodomains in annealed PIN ceramic. Note the fine contrast within each macrodomain, denoted X. (b) Dark-field image formed using a superstructure reflection, g of type 3/4, 3/4, 0 revealing antiferroelectric microdomains within the macrodomains.

are associated with regions of the PIN crystal which are in the antiferroelectric state. However, the dark regions are thought to be associated with non-antiferroelectric microdomains. Lattice imaging reveals that the antiferroelectric microdomains are aligned within the macro-twin domains. The dark regions are thought to be associated with the more disordered regions of the crystal and are thus expected to be in a relaxor ferroelectric phase. Further evidence that the partially ordered PIN has coexisting antiferroelectric and ferroelectric states is the presence of the β-type diffraction spots alongside the antiferroelectric superstructure spots, as already noted in Fig. 4.

4. Discussion

PIN is another complex perovskite material which can undergo a reversible order–disorder transition. The degree of order of the In and Nb B-site cations determines the dielectric characteristics of a given crystal or ceramic. In the disordered material there are significant chemical compositional fluctuations throughout the perovskite B-site sublattice, and these fluctuations imply that there is no unique Curie temperature but, instead, transitions occurring over a range of temperatures. This explanation for relaxor ferroelectric behaviour is known as the Smolenskii model and our observations appear to be consistent with it.

As disordered PIN (relaxor) is cooled, microregions undergo the paraelectric–ferroelectric soft mode transition and form polar microdomains. The superparaelectric model of Cross [8] suggests that the behaviour of the dipoles within each polar microdomain should depend on the size of the polar microdomains and their thermal energy. At high temperatures the dipoles may be fluctuating in orientation as a result of thermal agitations but lowering the temperature allows the dipoles to stabilize in crystallographically determined positions. We believe that the temperature-dependent nature explains why we have observed the stabilized microdomain structure at liquid nitrogen temperatures, where it is manifest as the mottled contrast, which has a scale of ~ 20 to 30 nm.

Annealing the PIN at 700° C allows the In^{+3} and Nb^{+5} cations to order on the B-site sublattice, a process which is driven by the electrostatic and strain energies within the material. The ordering of the indium and niobium cations also reduces the chemical fluctuations within the material and the spread of Curie temperatures is also reduced [12, 13]. In PIN there also appears to be a critical degree of B-site order at which the crystal transforms to an antiferroelectric phase at room temperature. Bokov *et al.* [22] discuss this change in terms of a thermodynamical description after coupling two free energies. These are a Landau free-energy term, which describes the ferroelectric (antiferroelectric) behaviour and a free-energy term from Bragg–Williams theory, which describes the B-site configurational energy. Rewriting these phenomological theories, Bokov *et al.* found that the Landau coefficients are quadratically dependent on the degree of order, and thus it is conceivable that the nature of the phase transitions is determined by the B-site order.

Another interesting aspect of PIN was discovered by Fenseko [23]. He characterized a number of $Pb(B'Nb)O_3$ perovskite compounds with B′ = Cr, Fe, Mn, Sc, In, Ln and Tm. Some of these compounds are ferroelectrics and some (B′ = Lu, Yb and Tm) are antiferroelectric. The changeover from ferroelectric to antiferroelectric behaviour occurs at the ionic radius possessed by both indium and scandium, so for PIN to show both antiferroelectric and ferroelectric characteristic is perhaps not a surprise. Coexisting antiferroelectric and ferroelectric phases are also to be expected within partially ordered PIN, because there should be regions where the local order is great enough to produce antiferroelectric PIN but when order is incomplete there may also be microdomains of ferroelectric PIN.

5. Conclusions

Disordered and ordered PIN ceramics and single crystals have been studied by TEM methods. In disordered PIN, a relaxor ferroelectric behaviour is observed whereas in the ordered PIN a "normal" antiferroelectric behaviour is observed. The observations are discussed in terms of the Smolenskii compositional model and analogies with superparamagnetic behaviour.

References

1. G. A. SMOLENSKII and V. A. ISUPOV, *Dokl. Akad. Nauk. SSSR* **9** (1954) 653.
2. G. A. SMOLENSKII and A. I. AGRANOVSKAJA, *Zh. tekh. Fiz.* **27** (1958) 2528.
3. G. A. SMOLENSKII, *J. Phys. Soc. Jpn (Suppl.)* **28** (1970) 26.
4. N. SETTER and L. E. CROSS, *J. Mater. Sci.* **15** (1980) 2478.
5. *Idem, J. Appl. Phys.* **51** (1980) 4356.
6. C. G. F. STENGER and A. BURGGRAAF, *Phys. Status. Solidi (a)* **61** (1980) 275.
7. *Idem*, **61** (1980) 653.
8. L. E. CROSS, Material Research Laboratory Annual report (1984).
9. L. E. CROSS, A. BHALLA and F. ASADIPOUS, *Amer. Ceram. Soc. Bull.* **65** (1986) 516.
10. YOKOSUKA and MURUTAKE, *Jap. J. Appl. Phys.* **25** (1986) 981.
11. A. V. TURIK, N. V. DOROKHOVA, N. B. SHEVCHENKO, K. R. CHERNYSHEV, M. F. KUPRIYANOV AND S. M. ZAITSEV, *Sov. Phys. Solid State* **22** (1980) 346.
12. A. A. BOKOV, I. P. RAEVSKII, V. G. SMOTRAKOV and I. M. TALYSHEVA, *Sov. Phys. Solid State* **26** (1984) 369.
13. P. GROVES, *J. Phys. C. Solid State Phys.* **19** (1986) 111.
14. *Idem, ibid.* **19** (1986) 5103.
15. A. V. TURIK, M. F. KUPRIYANOV, V. F. ZHESTKOV, N. B. SHEVCHENKO and V. A. KOGAN, *Sov. Phys. Solid State* **27** (1985), 1686.
16. S. SWARTZ and T. R. SHROUT, *Mater. Res. Bull.* **17** (1982) 1245.
17. P. GROVES, *Ferroelectrics* **65** (1985) 67.
18. C. A. RANDALL, D. J. BARBER, R. W. WHATMORE and P. GROVES, *J. Mater. Sci.* **21** (1986) 4456.
19. C. A. RANDALL, D. J. BARBER and R. W. WHATMORE, *J. Microscopy* **145** (1987) 275.
20. C. A. RANDALL, D. J. BARBER, P. GROVES and R. W. WHATMORE, *Ferroelectrics* **76** (1987) 311.
21. M. TANAKA, R. SAITO and K. TSUZUKI, *J. Appl. Phys.* **21** (1982) 291.
22. A. A. BOKOV, I. P. RAEVSKII and V. G. SMOTRAKOV, *Sov. Phys. Solid State* **25** (1983) 1168.
23. E. G. FENSENKO, "Perovskite Family and Ferroelectricity", (in Russian) (Atomizdat, Moscow, 1972).

Received 5 November 1987
and accepted 1 February 1988